Hindawi
Journal of Mathematics
Volume 2022, Article ID 6597924, 17 pages
https://doi.org/10.1155/2022/6597924

Review Article

Hall Current Effect of Magnetic-Optical-Elastic-Thermal-Diffusive Semiconductor Model during Electrons-Holes Excitation Processes

Abdulkafi M. Saeed,[1] **Kh. Lotfy**,[2,3] **and Alaa. A. El-Bary**[4,5,6]

[1]*Department of Mathematics, College of Science, Qassim University, P.O. Box 6644, Buraydah 51452, Saudi Arabia*
[2]*Department of Mathematics, Faculty of Science, Zagazig University, P.O. Box 44519, Zagazig, Egypt*
[3]*Department of Mathematics, Faculty of Science, Taibah University, Madinah, Saudi Arabia*
[4]*Arab Academy for Science, Technology and Maritime Transport, P.O. Box 1029, Alexandria, Egypt*
[5]*National Committee for Mathematics, Academy of Scientific Research and Technology, Cairo, Egypt*
[6]*Council of Future Studies and Risk Management, Academy of Scientific Research and Technology, Cairo, Egypt*

Correspondence should be addressed to Kh. Lotfy; khlotfy_1@yahoo.com

Received 4 September 2022; Accepted 1 November 2022; Published 15 November 2022

Academic Editor: M. M. Bhatti

In this study, a novel model is introduced when the Hall effect associated with a strong magnetic field is taken into account when the electrons and holes interact in the processes of semiconductor material. The plasma-elastic-thermal waves are investigated in the context of diffusive processes during optical-generated transport processes. The variable of thermal conductivity is obtained during graduated temperature due to the thermal impact of fallen light. The governing equations of the novel model are investigated in a unidimensional (1D) way when the electronics and elastic deformations have occurred. The Laplace transforms are used to convert the main dimensionless physical fields according to the initial conditions into the Laplace domain. When certain thermal, mechanical, holes, and electronic conditions are used, the analytical solutions of the fundamental fields can be produced to the outer surface of the semiconductor medium. Mathematically, the Laplacian computational inversion algorithm with a numerical approximation is used to achieve the fundamental physical quantities numerically in the time domain. The influences of several parameters (thermal relaxation times, Hall impact, and thermal conductivity parameters) on thermal conditions, mechanical stress, holes charge carrier field, and carrier density are prescribed with the help of graphical diagrams that are discussed theoretically.

1. Introduction

There are some materials with changing physical properties as temperature changes. Among these materials are semiconductors, as their characteristics are drastically altered by temperature fluctuations, particularly when light beams strike their surface. As a direct result of the thermal effect, the inner and outer atoms lose some electrons, which move rapidly toward the semiconductor's surface. The loss of electrons results in holes, which makes them in a state of diffusion and movement. This leads to a change in the resistance of the material because semiconductor's resistance lowers as temperature rises, which allows the passage of electric current. In this case and when studying semiconductors, thermal conductivity and its properties must be taken into consideration, as they depend on the temperature gradient. On the other hand, when semiconductor materials are exposed to a strong magnetic field, some internal physical changes occur, which affect the movement of both electrons and holes. Due to the magnetic fields and the thermal effect's existence, material deformation occurs, which lies in the thermal (thermoelastic) deformation (TED) resulting from the vibrations and collisions of the internal particles of the medium. For the other, it is electronic deformation (ED) (due to transport processes of electrons and holes)) as a result of the absorption of light energy on the surface, the accompanying processes of diffusion, and transfer of electrons and holes. Based on the above, electrons and holes are charge carriers adjacent to semiconductor materials.

When analyzing the changes that take place in the material's physical properties, the impact of Hall current caused by the strong magnetic field falling on semiconductor surfaces is crucial. The Hall effect was discovered when it was noted that electron concentration and position vary on a semiconductor when exposed to a magnetic field perpendicular to the current passage [1]. The strength of the magnetic field surrounding the particles and the current is directly related to the potential energy between them. The Hall effect is produced with the magnetic field's pressure force, which moves mobile holes and electrons. The Hall effect, created by the Hall current in semiconductor materials, can be used to analyze sample geometry and evaluate the positive and negative conductivity in a variety of applications, including mobile chargers.

The governing equations of the theory of thermoelasticity were used in the study of semiconductors as elastic materials. Numerous scientists discussed various models and how they can be applied to elastic materials. In the context of the generalized thermoelasticity theory (GET), Biot [2] introduced the coupled thermoelasticity (CT) theory, and then Lord and Ṣhulman (LS) [3] and Green and Lindsay (GL) [4] developed numerous models that rely on the influence of thermal and elastic relaxation durations to produce the physical fields. These models have demonstrated that waves propagating within elastic materials have finite velocity, which is consistent with observations and physics theories. On the other hand, numerous researchers have discussed a variety of physical properties of elastic materials using the overlap between the governing equations of GTE and two temperature theory with many applications [5–9]. The photothermal (PT) approach describes the interplay between various media's optical and thermal properties. It can be applied during the ED and TE deformations. On the other hand, Maruszewski [10] has developed the relationship between magnetic field (MF) waves and the thermodynamic characteristics of semiconductor medium.

The generalized photo-thermoelasticity theory (GPTET) can be used to express how elastic, thermal, and optical waves interact in semiconductor media. In recent years, many scientists have studied some models that describe the interference between elastic, thermal, and light waves when light beams fall on semiconductors during electron/hole diffusion [11, 12]. Sharma and Thakur [13] researched a novel model that describes the interaction between holes and electrons with the propagation of thermoelastic waves in a semiconductor medium. The photoacoustic sensitivity analysis is utilized during mass diffusion and heat transfer for semiconductor samples [14]. In contemporary technology, the photothermal (PT) approach is employed to ascertain the internal physical characteristics of semiconductors during the photo-excited transport processes [15]. The relationship between the PT theory and thermoelastic theory has been researched with several applications when the optical, thermal, and elastic properties are considered [16–19]. Lotfy et al. [20] and Mahdy et al. [21] investigated many problems when the Hall current influence of semiconductor materials is taken into consideration during electromagnetic field and laser pulse excitation processes when the thermal conductivity is independent of temperature. In the above studies, the effect of interaction between holes and electrons is neglected when the couple between photothermal and thermoelasticity theories is studied [22–24]. The Hall effect and the variable thermal conductivity are not studied during the coupled model of holes and electrons. Megahed et al. [25, 26] used some applications to study fluid properties utilizing thermal radiation. On the other hand, Gnaneswara Reddy and Ferdows [27, 28] studied Hall current, thermal radiation, and electro-magneto-hydrodynamic flow on microperistaltic channels with variable thermal conductivity.

In the framework of several photo-thermoelasticity models, the main goal of this work is to present a model that describes the interference between electrons and holes when the surface of a semiconductor is exposed to a strong magnetic field. Due to the strength of the magnetic field, the Hall current appears during optically excited diffusion processes in the medium. Working with a temperature gradient and variable thermal conductivity, the major findings of this article are discussed. Through the main governing equations, the model is studied in 1D deformation. The Laplace transform is utilized to obtain the analytical solutions from nondimensional fundamental physical fields (distributions of temperature strain, mechanical stress, and holes charge carrier field and plasma intensity). Some initial boundary conditions and the inversion of the Laplace technique are used with numerical approximation to achieve and determine the complete solutions in the time domain. The impacts of many parameters are illustrated graphically.

2. Governing Equation

(i) Based on the initial extremely powerful MF $\vec{H} = (0, H_0, 0)$ on the semiconductor rod in the direction of y-axis: In this case, the induced magnetic field $h_i = (0, h_2, 0) = (0, h, 0)$ is obtained. Here, the optical energy absorbed in the context of electronic/thermoelastic deformation's diffusive processes, the induced electric field $E_i = (0, 0, E)$, and the current density $J_r = (0, 0, J_3)$ are created perpendicular to $\vec{H}$ (see the schematic of the problem).

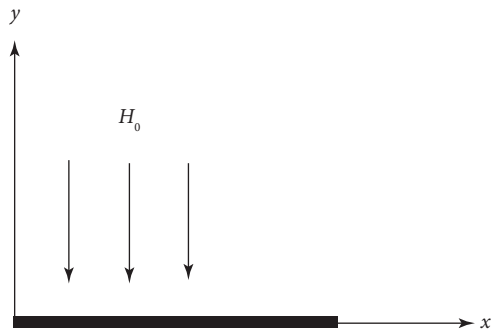

The Hall current is derived from the electromagnetic Ohm's equation, taking into account the strong external magnetic field pressure [29–32]:

$$\left.\begin{aligned} J_r &= \sigma_0\left(E_i + \mu_0\varepsilon_{ijr}\left(u_{j,t} - \frac{\mu_0}{en_e}J_j\right)H_r\right. \\ F_i &= \mu_0\varepsilon_{ijr}H_rJ_j,\ (i, j \text{ and } r = (1,2,3) = (x,y,z)) \end{aligned}\right\}. \quad (1)$$

The displacement tensor during the semiconductor medium is $u_j = (u_x, u_y, u_z)$, and μ_0 expresses the magnetic permeability. On the contrary, the velocity of the main particle can be represented as $u_{j,t}$. Due to the electronic deformation processes and magnetic field, the electrical conductivity $\sigma_0 = (n_e t_\xi e^2/m_e)$ is obtained, where e is the electron charge, m_e is the mass of the electron, n_e is the number density of electrons, t_ξ refers to the collision time between the electrons, and ε_{ijr} is the permutation symbol. However, the pressure force of the magnetic field can be determined by Lorentz force F_i. Due to a strong magnetic field, the induced electric field can be ignored, i.e., $E = 0$. According to ED and TED, the displacement quantity can be observed in 1D (the direction of x-axial). In this case, the displacement vector can be represented as $u_i = (u_x(x,t), 0, 0) = (u, 0, 0)$, with strain tensor $u_x = (\partial u/\partial x)$. Equation (1) allows for the extraction of the current density's constituents $J_1 = J_x = 0$ and $J_2 = J_y = 0$. The third component can be correlated with the displacement in the direction of z-axis as [20]

$$J_3 = J_z = \frac{\sigma_0\mu_0H_0}{1+m^2}\left(\frac{\partial u}{\partial t}\right). \quad (2)$$

The parameter of Hall current is $m = t_\xi\omega_e$ and the frequency of electron is $\omega_e = (e\mu_0H_0/m_e)$.

In this case, Lorentz's force $F_i = (F_x, 0, 0)$ can be rewritten as

$$F_x = \left(\frac{\sigma_0\mu_0^2H_0^2}{1+m^2}\right)\frac{\partial u}{\partial t}. \quad (3)$$

(ii) The homogeneity and isotropy of the medium are considered because of the photo-excited reactions that take place after the interaction between holes and electrons. The main fields in this problem are the carrier density (plasma wave) $N(x,t)$, the temperature (thermal wave) $T(x,t)$, and the hole charge carrier field $H(x,t)$ in addition to displacement $u(x,t)$. The following governing equations in 1D can be introduced [9] to represent the interference between thermal, elastic, and plasma (electrons and holes) waves in the absence of body forces and an internal heat source:

$$\left(1+\tau_\theta\frac{\partial}{\partial t}\right)\frac{\partial}{\partial x}\left[K\frac{\partial T}{\partial x}\right] + m_{nq}\frac{\partial^2 N}{\partial x^2} + m_{hq}\frac{\partial^2 H}{\partial x^2} - \rho\left(a_1^n\frac{\partial N}{\partial t} + a_1^h\frac{\partial H}{\partial t}\right) - \left(1+\tau_q\frac{\partial}{\partial t}\right)\left[\frac{K}{k}\frac{\partial T}{\partial t} + \rho T_0\alpha_n\frac{\partial N}{\partial t} + \rho T_0\alpha_h\frac{\partial H}{\partial t} + T_0\gamma\frac{\partial}{\partial x}\frac{\partial u}{\partial t}\right] = \left[\frac{\rho a_1^n}{t^n}N + \frac{\rho a_1^h}{t^h}H\right]\Bigg\}, \quad (4)$$

$$m_{qn}\frac{\partial^2 T}{\partial x^2} + D_n\rho\frac{\partial^2 N}{\partial x^2} - \rho\left(1 - a_2^nT_0\alpha_n + t^n\frac{\partial}{\partial t}\right)\frac{\partial N}{\partial t} - a_2^n\left[\frac{K}{k}\frac{\partial T}{\partial t} + \rho T_0\alpha_h\frac{\partial H}{\partial t} + T_0\gamma\frac{\partial}{\partial x}\frac{\partial u}{\partial t}\right] = -\frac{\rho}{t_1^n}\left(1 + t^n\frac{\partial}{\partial t}\right)N\Bigg\}, \quad (5)$$

$$m_{qh}\frac{\partial^2 T}{\partial x^2} + D_h\rho\frac{\partial^2 H}{\partial x^2} - \rho\left(1 - a_2^hT_0\alpha_h + t^h\frac{\partial}{\partial t}\right)\frac{\partial H}{\partial t} - a_2^h\left[\frac{K}{k}\frac{\partial T}{\partial t} + \rho T_0\alpha_n\frac{\partial N}{\partial t} + T_0\gamma\frac{\partial}{\partial t}\frac{\partial u}{\partial x}\right] = -\frac{\rho}{t_1^h}\left(1 + t^h\frac{\partial}{\partial t}\right)H\Bigg\}. \quad (6)$$

As shown below, Lorentz's force can be used to derive the equation of motion under the impact of Hall current [19, 20]:

$$\rho\frac{\partial^2 u}{\partial t^2} = (2\mu+\lambda)\frac{\partial^2 u}{\partial x^2} - \gamma\left(1+\tau_\theta\frac{\partial}{\partial t}\right)\frac{\partial T}{\partial x} - \delta_n\frac{\partial N}{\partial x} - \delta_h\frac{\partial H}{\partial x} - \left(\frac{\sigma_0\mu_0^2H_0^2}{1+m^2}\right)\frac{\partial u}{\partial t}. \quad (7)$$

Differentiating equation (7) relative to the component x yields [20]

$$\rho\frac{\partial^2 e}{\partial t^2}=(2\mu+\lambda)\frac{\partial^2 e}{\partial x^2}-\gamma\left(1+\tau_\theta\frac{\partial}{\partial t}\right)\frac{\partial^2 T}{\partial x^2}-\delta_n\frac{\partial^2 N}{\partial x^2}-\delta_h\frac{\partial^2 H}{\partial x^2}-\left(\frac{\sigma_0\mu_0^2H_0^2}{1+m^2}\right)\frac{\partial e}{\partial t}, \tag{8}$$

where $a_1^n=(a_{Qn}/a_Q)$, $a_1^h=(a_{Qh}/a_Q)$, $a_2^n=(a_{Qn}/a_n)$, $a_2^h=(a_{Qh}/a_h)$, and $(\rho C_e/K)=(1/k)$ represents the thermal viscosity. The constitutive equation during the 1D deformation when the interaction between electrons and holes is taken into consideration and can be expressed as follows:

$$\sigma_{xx}=\sigma=-\left(\gamma\left(1+\tau_\theta\frac{\partial}{\partial t}\right)T+\delta_nN+\delta_hH\right)+(2\mu+\lambda)e. \tag{9}$$

(iii) The increase in the temperature of semiconductors causes internal deformations of the material, which affects its physical properties. The most important quantity inside a material that is affected by the temperature gradient is thermal conductivity [23, 24]. Therefore, thermal conductivity can be described as a temperature-dependent linear function of temperature, which can be written as follows:

$$K(T)=K_0(1+K_\theta T). \tag{10}$$

In a semiconductor medium, the parameter K_0 is the thermal conductivity when $K_\theta=0$, and K_θ can be taken as a small nonpositive parameter [32]. The mapping technique is used to obtain the relation between temperature and thermal conductivity, which is defined as follows:

$$\Theta=\frac{1}{K_0}\int_0^T K(\vartheta)\mathrm{d}\vartheta. \tag{11}$$

Operating equation (11) by $(\partial/\partial x)$ and $(\partial/\partial t)$ yields

$$\left.\begin{aligned}K_0\frac{\partial\Theta}{\partial x}&=K(T)\frac{\partial T}{\partial x}\\ K_0\frac{\partial\Theta}{\partial t}&=K(T)\frac{\partial T}{\partial t}\end{aligned}\right\}. \tag{12}$$

Therefore, neglecting nonlinear terms (the medium is linear) yields

$$K_0\frac{\partial\Theta}{\partial x}=K(T)\frac{\partial T}{\partial x}\Rightarrow\text{when differentiating both sides by}\frac{\partial}{\partial x}\Rightarrow\frac{\partial}{\partial x}\left(K_0\frac{\partial\Theta}{\partial x}\right)=\frac{\partial}{\partial x}\left(K(T)\frac{\partial T}{\partial x}\right)=K_0K_\theta\left\{\left(\frac{\partial T}{\partial x}\right)^2+\frac{\partial^2T}{\partial x^2}\right\}=K_0K_\theta\frac{\partial^2T}{\partial x^2}\Bigg\}, \tag{13}$$

$$\frac{\partial}{\partial x}\left(K\frac{\partial T}{\partial x}\right)=\frac{\partial}{\partial x}\left(K_0(1+K_\theta T)\frac{\partial T}{\partial x}\right)=K_0\frac{\partial^2\Theta}{\partial x^2}+K_0K_\theta\left[\frac{\partial\Theta}{\partial x}\right]^2=K_0\frac{\partial^2\Theta}{\partial x^2}, \tag{14}$$

$$\frac{K_0}{K}\frac{\partial\Theta}{\partial x}=\frac{K_0}{K_0(1+K_\theta T)}\frac{\partial\Theta}{\partial x}=\left({}_1\frac{\partial\Theta}{\partial x}\right)=\left(1-K_\theta T+(K_\theta-\cdots)\frac{\partial\Theta}{\partial x}\right)=\frac{\partial\Theta}{\partial x}-K_\theta T\frac{\partial\Theta}{\partial x}+\left({}_{K_\theta}\frac{\partial\Theta}{\partial x}-\cdots\right)=\frac{\partial\Theta}{\partial x}\Bigg\}. \tag{15}$$

Using the above map transformations equations (10)–(12) and (13)–(15) of the basic equations (4)–(7) yields

$$\begin{aligned}&\left(1+\tau_\theta\frac{\partial}{\partial t}\right)\frac{\partial}{\partial x}\left[K_0\frac{\partial\Theta}{\partial x}\right]+m_{nq}\frac{\partial^2N}{\partial x^2}+m_{hq}\frac{\partial^2H}{\partial x^2}-\rho\left(a_1^n\frac{\partial N}{\partial t}+a_1^h\frac{\partial H}{\partial t}\right)\\ &\quad-\left(1+\tau_q\frac{\partial}{\partial t}\right)\left[\frac{K_0}{k}\frac{\partial\Theta}{\partial t}+\rho T_0\alpha_n\frac{\partial N}{\partial t}+\rho T_0\alpha_h\frac{\partial H}{\partial t}+T_0\gamma\frac{\partial}{\partial x}\frac{\partial u}{\partial t}\right]=\left[\frac{\rho a_1^n}{t^n}N+\frac{\rho a_1^h}{t^h}H\right]\Bigg\},\end{aligned} \tag{16}$$

$$\frac{m_{qn}}{K_\theta}\frac{\partial^2\Theta}{\partial x^2}+D_n\rho\frac{\partial^2N}{\partial x^2}-\rho\left(1-a_2^nT_0\alpha_n+t^n\frac{\partial}{\partial t}\right)\frac{\partial N}{\partial t}-a_2^n\left[\frac{K_0}{k}\frac{\partial\Theta}{\partial t}+\rho T_0\alpha_h\frac{\partial H}{\partial t}+T_0\gamma\frac{\partial}{\partial x}\frac{\partial u}{\partial t}\right]=-\frac{\rho}{t_1^n}\left(1+t^n\frac{\partial}{\partial t}\right)N\Bigg\}, \tag{17}$$

$$\frac{m_{qh}}{K_\theta}\frac{\partial^2\Theta}{\partial x^2}+D_h\rho\frac{\partial^2 H}{\partial x^2}-\rho\left(1-a_2^hT_0\alpha_h+t^h\frac{\partial}{\partial t}\right)\frac{\partial H}{\partial t}-a_2^h\left[\frac{K_0}{k}\frac{\partial\Theta}{\partial t}+\rho T_0\alpha_n\frac{\partial N}{\partial t}+T_0\gamma\frac{\partial}{\partial t}\frac{\partial u}{\partial x}\right]=-\frac{\rho}{t_1^h}\left(1+t^h\frac{\partial}{\partial t}\right)H\Bigg\}, \tag{18}$$

$$\rho\frac{\partial^2 e}{\partial t^2}=(2\mu+\lambda)\frac{\partial^2 e}{\partial x^2}-\gamma\left(1+\tau_\theta\frac{\partial}{\partial t}\right)\frac{\partial^2\Theta}{\partial x^2}-\delta_n\frac{\partial^2 N}{\partial x^2}-\delta_h\frac{\partial^2 H}{\partial x^2}-\left(\frac{\sigma_0\mu_0^2H_0^2}{1+m^2}\right)\frac{\partial e}{\partial t}. \tag{19}$$

The addition of the dimensionless quantities listed below makes matters more appropriate:

$$\left.\begin{aligned}
&(x\prime,u\prime)=\frac{\omega^*(x,u)}{C_T}\\
&\left(t\prime,\tau_q',\tau_\theta',t^{n\prime},t^{h\prime},t_1^{h'},t_1^{h}\right)=\omega^*\left(t,\tau_q,\tau_\theta,t^n,t^h,t_1^n,t_1^h\right)\\
&\beta^2=\frac{C_T^2}{C_L^2}\\
&k=\frac{K}{\rho C_e}\\
&\sigma_{ij}'=\frac{\sigma_{ij}}{2\mu+\lambda}\\
&N\prime=\frac{\delta_n(N)}{2\mu+\lambda}\\
&C_T^2=\frac{2\mu+\lambda}{\rho}\\
&C_L^2=\frac{\mu}{\rho}\\
&\omega^*=\frac{C_e(\lambda+2\mu)}{K}\\
&\left(\overline{\delta}_n,\overline{\delta}_h\right)=\frac{(\delta_n n_0,\delta_h h_0)}{\gamma T_0}\\
&\Theta\prime=\frac{\gamma(\Theta)}{2\mu+\lambda}\\
&H\prime=\frac{\delta_n(H)}{2\mu+\lambda}
\end{aligned}\right\}. \tag{20}$$

Using equation (20) with ignoring the dashes for more appropriateness, the main equations (7), (8), and (16)–(19) yield

$$\left\{\left(1+\tau_\theta\frac{\partial}{\partial t}\right)\frac{\partial^2}{\partial x^2}-\left(1+\tau_q\frac{\partial}{\partial t}\right)\frac{\partial}{\partial t}\right\}\Theta+\left\{\alpha_1\frac{\partial^2}{\partial x^2}-\alpha_2\left(1+\tau_q\frac{\partial}{\partial t}\right)-\alpha_3\frac{\partial}{\partial t}-\alpha_4\right\} N+\left\{\alpha_5\frac{\partial^2}{\partial x^2}-\left(1+\tau_\alpha\frac{\partial}{\partial t}\right)\alpha_6-\alpha_7\right\}H-\left(1+\tau_q\frac{\partial}{\partial t}\right)\varepsilon_1\frac{\partial e}{\partial t}=0\Bigg\}, \tag{21}$$

$$\left\{\frac{\partial^2}{\partial x^2}-\alpha_8\frac{\partial}{\partial t}\right\}\Theta+\left\{\alpha_9\frac{\partial^2}{\partial x^2}-\left(\alpha_{10}+t^n\frac{\partial}{\partial t}\right)\alpha_{11}+\left(1+t^n\frac{\partial}{\partial t}\right)\frac{\alpha_{11}}{t^n}\right\}N-\alpha_{12}\frac{\partial H}{\partial t}-\alpha_{13}\frac{\partial e}{\partial x}=0\Bigg\}, \tag{22}$$

$$\left\{\frac{\partial^2}{\partial x^2}-\alpha_{18}\frac{\partial}{\partial t}\right\}\Theta+\left\{\alpha_{14}\frac{\partial^2}{\partial x^2}-\left(\alpha_{15}+t^h\frac{\partial}{\partial t}\right)\alpha_{16}\frac{\partial}{\partial t}+\left(1+t^h\frac{\partial}{\partial t}\right)\alpha_{17}\right\}H-\alpha_{19}\frac{\partial N}{\partial t}-\alpha_{20}\frac{\partial e}{\partial t}=0\Bigg\}, \tag{23}$$

$$\left(\frac{\partial^2}{\partial x^2}-\frac{\partial^2}{\partial t^2}-\frac{M}{1+m^2}\frac{\partial}{\partial t}\right)e-\left(1+\tau_\theta\frac{\partial}{\partial t}\right)\frac{\partial^2\Theta}{\partial x^2}-\frac{\partial^2 N}{\partial x^2}-\alpha_{21}\frac{\partial^2 H}{\partial x^2}-\left(\frac{\sigma_0\mu_0^2H_0^2}{1+m^2}\right)\frac{\partial e}{\partial t}, \tag{24}$$

$$\sigma=\left(e-\left(\left(1+\tau_\theta\frac{\partial}{\partial t}\right)\Theta+N\right)\right)-H. \tag{25}$$

In this case, the strength of the magnetic pressure number can be obtained by $M=(\sigma_0 t^*\mu_0^2H_0^2/\rho)$ which refers to the Hartmann number. The other coefficients are $\alpha_1=(m_{nq}\alpha_t/d_nK_0)$, $\alpha_2=(T_0\alpha_n/C_e)$, $\alpha_3=(a_1^n/C_e)$, $\alpha_4=(a_1^n\gamma/C_e\tau^n\ (2\mu+\lambda))$, $\alpha_5=(\gamma m_{hq}h_0/(2\mu+\lambda)K_0)$, $\alpha_6=(T_0\alpha_hK_0h_0/C_e)$, $\alpha_7=(a_1^h\gamma\omega^*/t^hK_0)$, $\alpha_8=(a_2^nK_1/m_{qn})$, $\alpha_9=(D_nh_0\gamma/C_T^2m_{qh})$, $\alpha_{10}=1-a_2^nT_0\alpha_n$, $\alpha_{11}=(\alpha_tK_0/m_{qn}d_nC_e)$, $\alpha_{12}=(a_2^n\gamma h_0\alpha_h\omega^*/m_{qn})$, $\alpha_{13}=(a_2^n\gamma^2T_0\omega^*/\rho m_{qn})$, $\alpha_{14}=(D_nh_0\gamma/C_T^2m_{qh})$, $\alpha_{15}=1-a_2^hT_0\alpha_n$, $\alpha_{16}=(\gamma h_0\omega^*/m_{qh})$, $\alpha_{17}=(\gamma h_0\omega^*/m_{qh}\tau_1^h)$, $\alpha_{18}=a_2^h(K_1/m_{qh})$, $\alpha_{19}=(a_2^h\gamma T_0\alpha_n(2\mu+\lambda)\omega^*/m_{qh}\delta_n)$, $\alpha_{20}=(a_2^h\gamma^2T_0\omega^*/m_{qh}\rho)$, $\alpha_{21}=(\delta_h/(2\mu+\lambda))$, and $\varepsilon_1=(T_0\gamma^2\omega^*/\rho K_0)$.

The values α_1 and α_{21} represent the optical-elastic-thermal coupling parameters, and ε_1 is the thermoelastic coupling parameter.

The following initial conditions are supposed when the medium is homogeneous at $x=0.0$, which are can be written as

$$\begin{aligned} e(x,t)|_{t=0}&=\frac{\partial e(x,t)}{\partial t}\Big|_{t=0}=0,\\ T(x,t)|_{t=0}&=\frac{\partial T(x,t)}{\partial t}\Big|_{t=0}=0,\\ H(x,t)|_{t=0}&=\frac{\partial H(x,t)}{\partial t}\Big|_{t=0}=0,\\ N(x,t)|_{t=0}&=\frac{\partial N(x,t)}{\partial t}\Big|_{t=0}=0. \end{aligned} \tag{26}$$

3. Analytical Solution Procedure

The Laplace transform technique with a parameter s can be employed with the parameter s for the governing equations, which can be formulated for function $\Upsilon(x,t)$ as

$$L(\phi(x,t))=\int_0^\infty e^{-st}\phi(x,t)\mathrm{d}t=\overline{\phi}(x,s). \tag{27}$$

Using Laplace transform equation (27) with the initial conditions for the main system (21)–(25) yields

$$\left(q_1D^2-q_2\right)\overline{\Theta}+\left(\alpha_1D^2-q_3\right)\overline{N}+\left(\alpha_5D^2-q_4\right)\overline{H}-q_5\overline{e}=0, \tag{28}$$

$$\left(D^2-q_7\right)\overline{\Theta}+\left(\alpha_9D^2-q_6\right)\overline{N}-q_8\overline{H}-q_9\overline{e}=0, \tag{29}$$

$$\left(D^2-q_{10}\right)\overline{\Theta}+\left(\alpha_{14}D^2-q_{11}\right)\overline{H}-q_{12}\overline{N}-q_{13}\overline{e}=0, \tag{30}$$

$$\left(D^2-\mathfrak{R}_H\right)\overline{e}-q_{14}D^2\overline{\Theta}-D^2\overline{N}-\alpha_{21}^*D^2\overline{H}=0, \tag{31}$$

$$\overline{\sigma}=\alpha_{23}\left(\overline{e}-\left((1+s\tau_\theta)\overline{\Theta}+\overline{N}\right)\right)-\overline{H}, \tag{32}$$

where $D=(\mathrm{d}/\mathrm{d}x)$, $q_1=(1+\tau_\theta(\partial/\partial t))$, $\mathfrak{R}_H=s^2+s(M/(1+m^2))$, $q_2=(1+\tau_q(\partial/\partial t))s$, $q_4=(1+\tau_q(\partial/\partial t))\alpha_6+\alpha_7$, $q_3=(\alpha_2(1+\tau_q(\partial/\partial t))+\alpha_3(\partial/\partial t)+\alpha_4)$, $q_6=(\alpha_{10}+t^ns)\alpha_{11}-(1+t^ns)(\alpha_{11}/t^n)$, $\alpha_{21}^*=(\delta_h/(2\mu+\lambda))$, and $q_5=(1+\tau_qs)\varepsilon_1s$, $q_7=\alpha_8s$, $q_8=\alpha_{12}s$, $q_{12}=\alpha_{19}s$, $q_{13}=\alpha_{20}s$, $q_{14}=1+\tau_\theta s$, $q_9=\alpha_{13}s$, $q_{10}=\alpha_{18}s$, $q_{11}=(\alpha_{15}+t^hs)\alpha_{16}s-(1+t^hs)\alpha_{17}$.

To solve the derived system of the governing equations (28)–(31), the elimination method is used in terms of $\overline{\Theta},\overline{e},\overline{N}$, and $\overline{H}$ to obtain

$$\left(D^8-\Xi_1D^6+\Xi_2D^4-\Xi_3D^2+\Xi_4\right)\{\overline{H},\overline{N},\overline{\Theta},\overline{e}\}(x,s)=0. \tag{33}$$

The main coefficients of the above equation can be obtained with the help of the software computer, which takes the form as follows:

Table 1: The physical input parameters of Si material in SI units.

Unit	Symbol	Value
N/m^2	λ	6.4×10^{10}
	μ	6.5×10^{10}
kg/m^3	ρ	2330
K	T_0	800
Sec (s)	τ	5×10^{-5}
K^{-1}	α_t	4.14×10^{-6}
$Wm^{-1}\cdot K^{-1}$	k	150
J/(kg·K)	C_e	695
m^2/s	D_e	2.5×10^{-3}
m/s	$\overline{s}$	2
H/m	μ_0	$4\pi\times10^{-7}$
$Col^2/Cl\cdot cm\cdot s$	σ_0	9.36×10^{5}
	m_{qn}	1.4×10^{-5}
vk^{-1}	m_{nq}	1.4×10^{-5}
	m_{qh}	-0.004×10^{-6}
	m_{hq}	-0.004×10^{-6}
m^2s^{-1}	D_n	0.35×10^{-2}
m^2s^{-1}	D_h	0.125×10^{-2}
m^2/s	α_n	1×10^{-2}
m^2/s	α_h	5×10^{-3}
m/s	$\overline{\lambda}$	2
m^{-3}	n_0	10^{20}
m^{-3}	h_0	10^{20}

$$\Xi_1 = \frac{-1}{(\alpha_9\alpha_{14}q_1 - \alpha_1\alpha_{14} - \alpha_5\alpha_9)}\left(\alpha_{14}q_1\left(\mathfrak{R}_H\alpha_9 - \alpha_1q_{14}\right) + \alpha_9q_{14}\left(\alpha_5q_{13} + \alpha_{14}q_5\right) + \alpha_{21}^*\alpha_9q_{13}q_1 - \alpha_1\alpha_{14}\left(\mathfrak{R}_H + q_7\right) - \alpha_1\alpha_{21}^*q_9 - \alpha_9q_4 - \alpha_1\alpha_{21}^*q_{13}\right.$$
$$\left. - \alpha_5\alpha_9q_{10} + \alpha_{14}\alpha_9q_2 - \alpha_9\alpha_{21}^*q_5 + \alpha_9q_1q_{11} + \alpha_{14}q_1q_6 + q_6\left(\alpha_{14}q_1 - \alpha_5\right) - \alpha_1\left(q_{11} - q_8\right) + \alpha_5\left(q_{12} + q_{13}\right) - \alpha_{14}\left(q_3 + q_5\right)\right)\},$$

$$\Xi_2 = \frac{-1}{(\alpha_9\alpha_{14}q_1 - \alpha_1\alpha_{14} - \alpha_5\alpha_9)}\left(\mathfrak{R}_H\left(\alpha_9q_{14}q_1 + \alpha_9\left(\alpha_5q_{10} - \alpha_{14}q_2 - q_1q_{11}\right) - \alpha_{14}q_1q_6\right) + \alpha_1\left(\alpha_{21}q_7q_{13} - \alpha_{21}^*q_9q_{10} - q_{14}\left(q_8q_{13} - q_9q_{11}\right)\right) + \alpha_5q_{14}\left(q_6q_{13} - q_9q_{12}\right)\right.$$
$$- \alpha_9\alpha_{21}^*\left(q_2q_{13} - q_5q_{10}\right) + \alpha_9q_{14}\left(q_4q_{13} - q_5q_{11}\right) + \alpha_{14}q_{14}\left(q_3q_9 - q_5q_6\right) - \alpha_{21}^*q_1\left(q_6q_{13} - q_9q_{12}\right) - \mathfrak{R}_H\left(\alpha_1\left(q_8 - q_{11}\right) + \alpha_5q_{12} - \alpha_9q_4 - \alpha_{14}q_3\right)$$
$$+ \alpha_1\left(q_7q_{11} - q_8q_{10}\right) + \alpha_5\left(q_6q_{10} - q_7\left(q_{12} + q_{13}\right) + q_9q_{10}\right) - \alpha_9\left(q_2q_{11} - q_4q_{10}\right) - \alpha_{14}\left(q_2\left(q_6 - q_9\right) - q_7\left(q_3 + q_7\right)\alpha_{21}^*\left(q_3q_{13} - q_5\left(q_6 + q_{12}\right)\right)\right)$$
$$\left. - q_1\left(q_6q_{11} - q_8\left(q_{12} - q_{13}\right) + q_9q_{11}\right) - q_3\left(q_8 - q_{11}\right) - q_4\left(q_6 + q_9 - q_{12} + q_{13}\right) + q_5\left(q_8 - q_{11}\right)\right)\},$$

$$\Xi_3 = \frac{-1}{(\alpha_9\alpha_{14}q_1 - \alpha_1\alpha_{14} - \alpha_5\alpha_9)}\left\{\mathfrak{R}_H\left(\alpha_1q_8q_{10} - \alpha_1q_7q_{11} - \alpha_5q_6q_{10} + \alpha_5q_7q_{12} + \alpha_9\left(q_2q_{11} - q_4q_{10}\right) + \alpha_{14}\left(q_2q_6 - q_3q_7\right) + q_1\left(q_6q_{11} - q_8q_{12}\right)\right) + \alpha_{21}^*\left(q_2\left(q_6q_{13} - q_9q_{12}\right)\right.\right.$$
$$\left. - q_3\left(q_7q_{13} - q_9q_{10}\right) - q_5\left(q_6q_{10} - q_7q_{12}\right)\right) + q_3q_{14}\left(q_8q_{13} - q_9q_{11}\right) - q_4q_{14}\left(q_6q_{13} - q_9q_{12}\right) - q_5q_{14}\left(q_6q_{11} - q_8q_{12}\right) + \mathfrak{R}_H\left(q_3\left(q_8 - q_{11}\right) - q_4\left(q_6 - q_{12}\right)\right)$$
$$\left. + q_2\left(q_6q_{11} - q_8q_{12} - q_8q_{13} + q_9q_{11}\right) - q_3\left(q_7q_{11} - q_8q_{10}\right) - q_4\left(q_6q_{10} - q_7\left(q_{12} + q_{13}\right) + q_9q_{10}\right) + q_5\left(q_8q_{10} - q_8q_{10}\right)\right\},$$

$$\Xi_4 = \left.\frac{\mathfrak{R}_H\left(-q_2q_6q_{11} + q_2q_8q_{12} + q_3\left(q_7q_{11} - q_8q_{10}\right)q_4\left(q_6q_{10} - q_7q_{12}\right)\right)}{\left(-\alpha_9\alpha_{14}q_1 + \alpha_1\alpha_{14} + \alpha_5\alpha_9\right)}\right\}. \tag{34}$$

Equation (33) is factorized as

$$\left(D^2 - m_1^2\right)\left(D^2 - m_2^2\right)\left(D^2 - m_3^2\right)\left(D^2 - m_4^2\right)\{\overline{N}, \overline{H}, \overline{T}, \overline{e}\}(x, s) = 0, \tag{35}$$

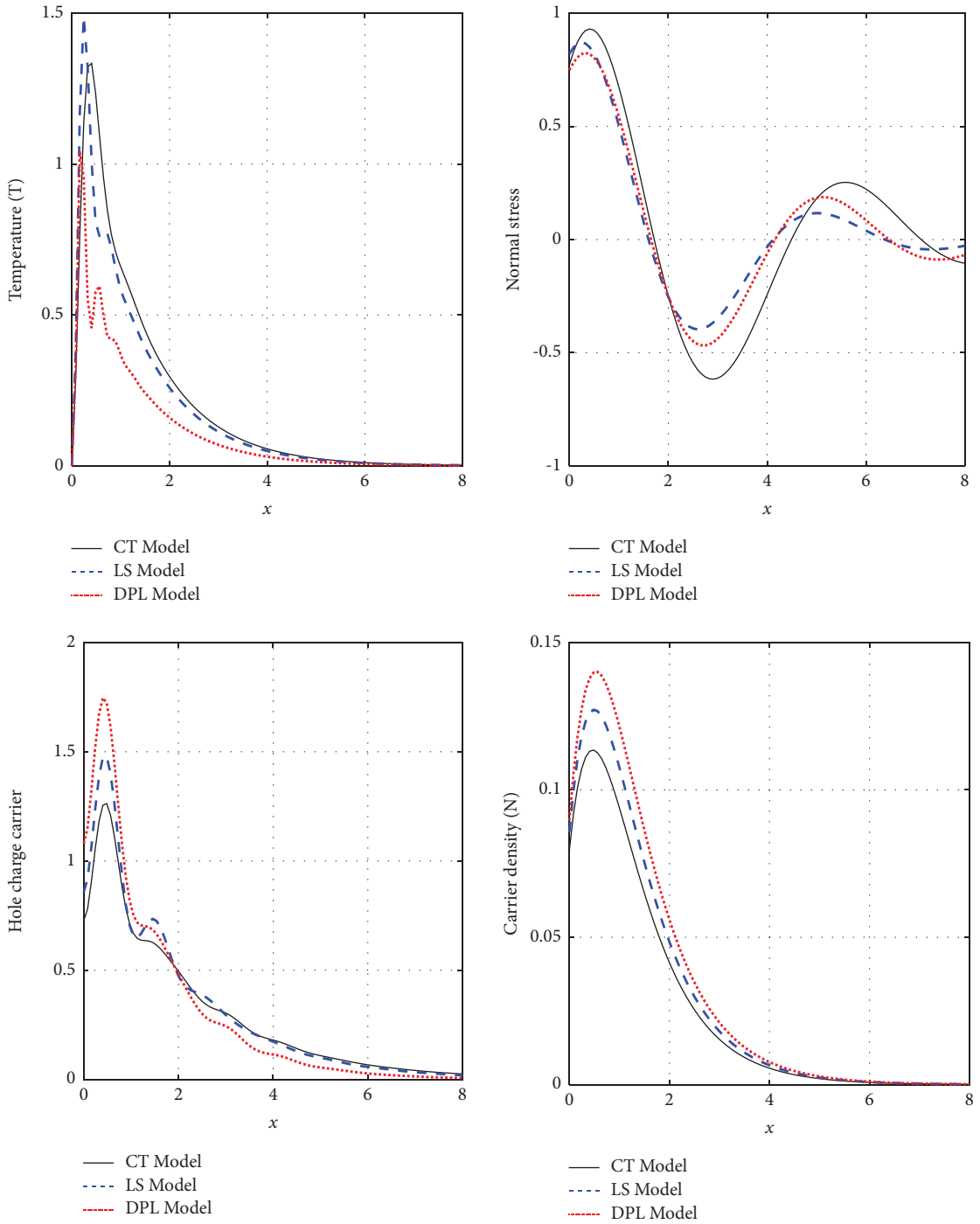

Figure 1: The variation of the main physical distributions against the distance according to photo-thermoelasticity models with variable thermal conductivity under the effect of Hall current.

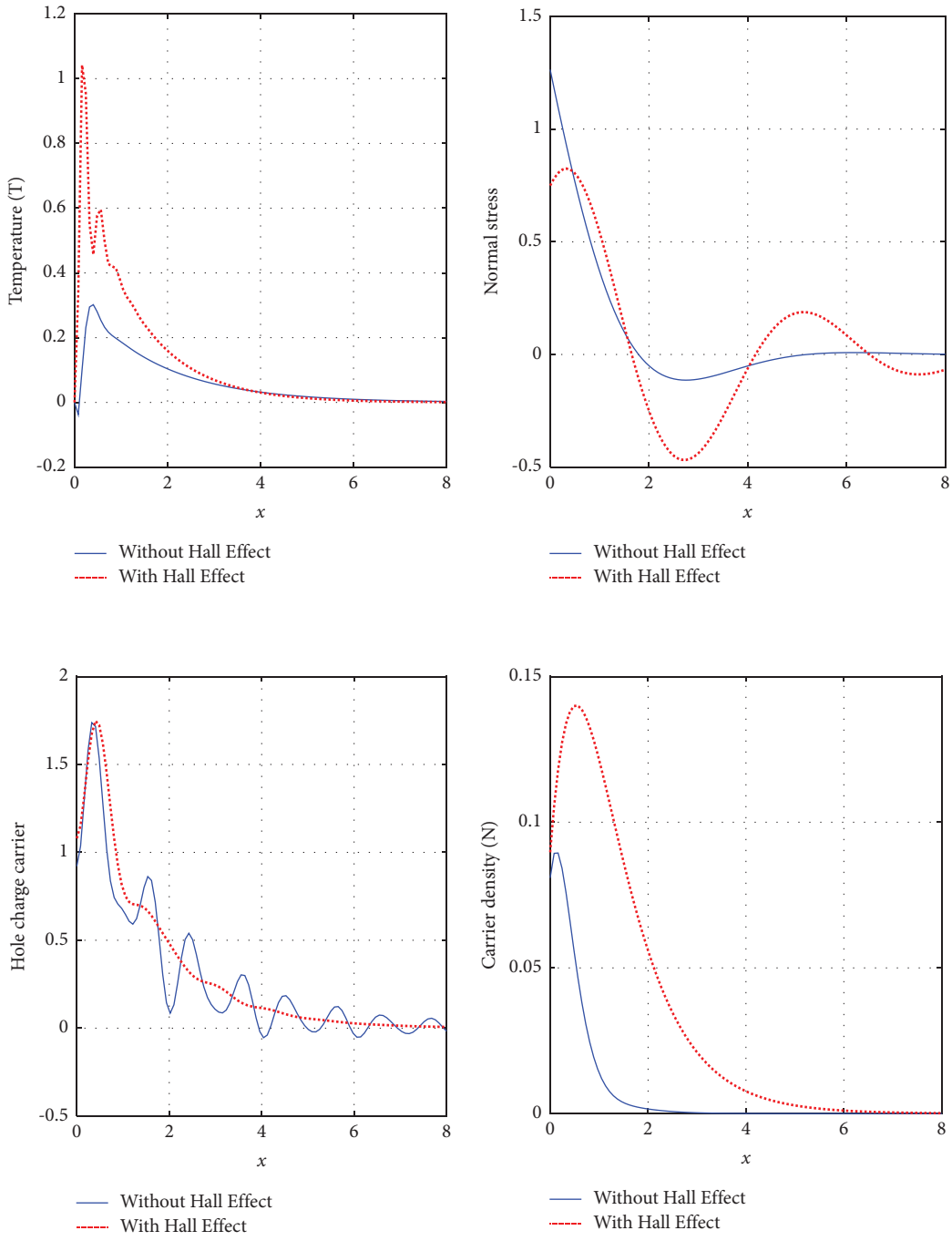

Figure 2: The variation of physical fields verses the axial distance according to the DPL model with variable thermal conductivity in the absence and presence of Hall current.

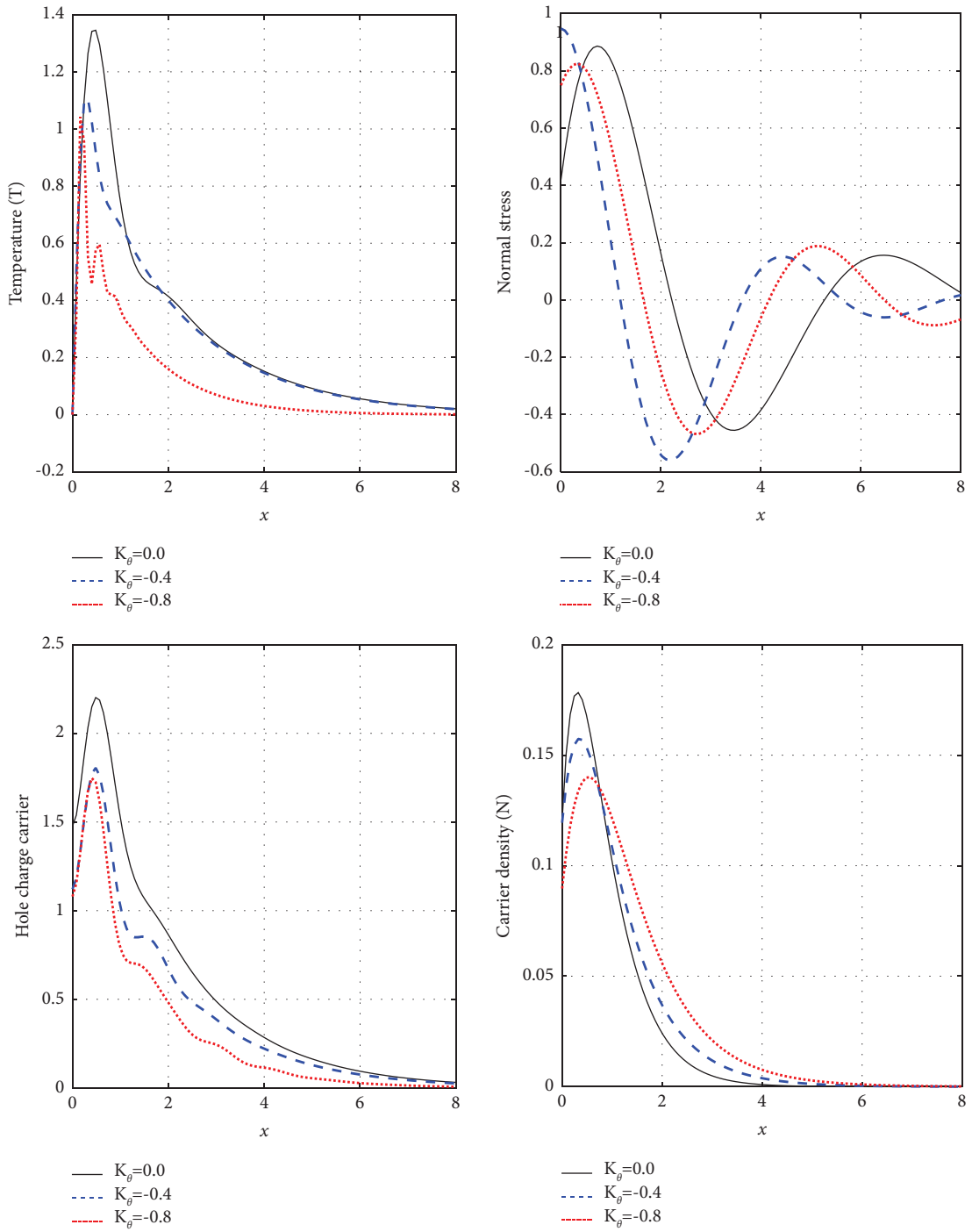

Figure 3: The variation of the physical field distributions verses the axial distance in three cases of thermal conductivity under the impact of Hall current according to the DPL model.

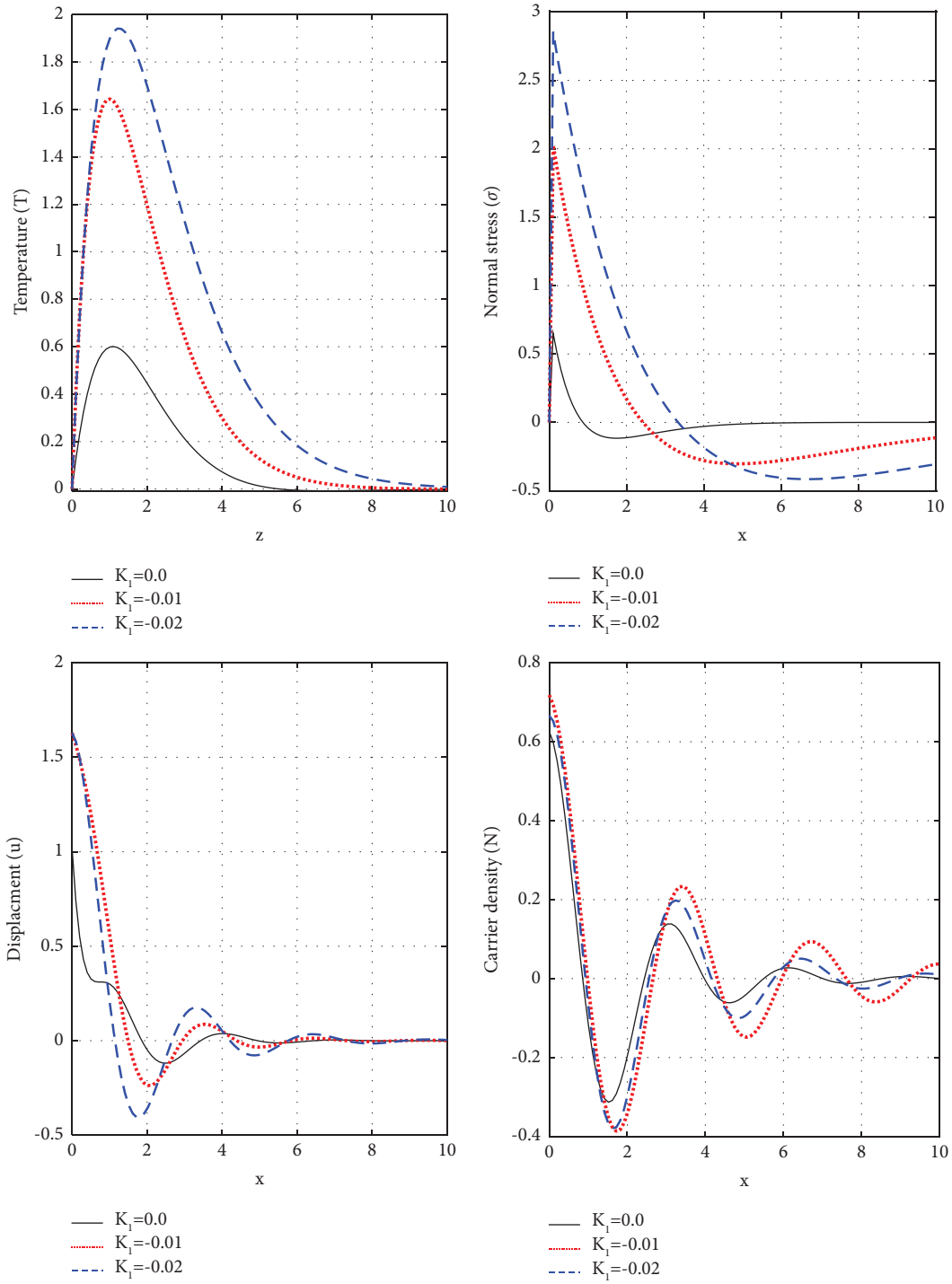

FIGURE 4: The variation of physical fields verses the axial distance according to the DPL model with variable thermal conductivity in the absence of holes carrier charge field.

where m_1^2, m_2^2, m_3^2, and m_4^2 are the roots of the characteristic equation of equation (35) at $x \longrightarrow \infty$. Therefore, when the waves are propagated in the axial direction, the real roots with positive amplitude can be chosen. The linear solutions of the physical fields in the Laplace domain can be written as

$$\begin{aligned}
\overline{\Theta}(x,s) &= \sum_{i=1}^{4} B_i(s)e^{-m_i x},\\
\overline{N}(x,s) &= \sum_{i=1}^{4} B_i'(s)e^{-m_i x} = \sum_{i=1}^{4} H_{1i}B_i(s)e^{-m_i x},\\
\overline{e}(x,s) &= \sum_{i=1}^{4} B_i''(s)e^{-m_i x} = \sum_{i=1}^{4} H_{2i}B_i(s)e^{-m_i x},\\
\overline{H}(x,s) &= \sum_{i=1}^{4} B_i''(s)e^{-m_i x} = \sum_{i=1}^{4} H_{3i}B_i(s)e^{-m_i x},\\
\overline{\sigma}(x,s) &= \sum_{i=1}^{4}\left(B_i'''(s)\right)e^{-m_i x} = \sum_{i=1}^{4}\left(H_{4i}B_i(s)\right)e^{-m_i x},
\end{aligned} \tag{36}$$

where the main coefficients are

$$\left.\begin{aligned}
H_{1i} &= -\frac{\alpha_{14}m_i^6 + c_7 m_i^4 + c_8 m_i^2 + c_9}{\alpha_9\alpha_{14}m_i^6 + c_4 m_i^4 + c_5 m_i^2 + c_6}\\
H_{2i} &= \frac{c_{10}m_i^6 + c_{11}m_i^4 + c_{12}m_i^2}{\alpha_9\alpha_{14}m_i^6 + c_4 m_i^4 + c_5 m_i^2 + c_6}\\
H_{3i} &= -\frac{\alpha_9 m_i^6 + c_1 m_i^4 + c_2 m_i^2 + c_3}{\alpha_9\alpha_{14}m_i^6 + c_4 m_i^4 + c_5 m_i^2 + c_6}\\
H_{4i} &= \alpha_{23}\left(H_{2i} - \left((1+s\tau_\theta)H_{1i} + 1\right) - \alpha_{22}H_{3i}\right)
\end{aligned}\right\}. \tag{37}$$

4. Applications (Mechanical Ramp Type)

The medium's free surface, $x = 0$, is subjected to mechanical ramp type, thermal, and plasma conditions to ascertain the value of the unidentified parameters B_i. However, the conditions can be written as follows:

(i) The medium can be chosen in the isothermal type at $x = 0$ with Laplace transform, which can be represented as [23, 24]

$$\overline{\Theta}(0,s) = 0 \Rightarrow\Rightarrow \sum_{n=1}^{4} B_i(s) = 0. \tag{38}$$

(ii) The mechanical ramp type at the free surface $x = 0$ can be applied, which can be formulated for the normal stress component as [24]

$$\sigma(x,t) = \begin{cases} 0, & t \le 0,\\ \dfrac{t}{t_0}, & 0 < t \le t_0,\\ 1, & t > t_0. \end{cases} \tag{39}$$

In the Laplace domain, the normal stress can be rewritten as

$$\sum_{i=1}^{4} H_{4i}B_i(s) = \overline{F}(s)\frac{\left(1 - e^{-st_0}\right)}{t_0 s^2}. \tag{40}$$

(iii) The condition of plasma wave can be applied at the surface $x = 0$ when the carrier density propagates during the recombination processes when the medium is excited with mass and heat transfer. However, under the effect of the Laplace transform, this condition can be written [24] as

$$\overline{N}(0,s) = \frac{\tilde{s}\lambda n_0}{D_e} \Rightarrow\Rightarrow \sum_{i=1}^{4} H_{1i}B_i(s) = \frac{\lambda\tilde{s}n_0}{D_e}. \tag{41}$$

(iv) The recombination diffusion for the hole charge field during the optical-excitation processes at the surface $x = 0$ occurs and can be written under the Laplace transform in the equilibrium case [20] as

$$\overline{H}(0,s) = h_0 \Rightarrow\Rightarrow \sum_{i=1}^{4} H_{3i}B_i(s) = h_0, \tag{42}$$

where $\tilde{s}$ is the recombination speed, D_e is the electron charge diffusion coefficient, and λ is a chosen (positive) parameter. Using the thermal, mechanical, plasma, and holes boundary condition equations (38) and (40)–(42), the unknown coefficient $B_i(s)$ can be calculated [30].

5. Processes of the Laplace Transform Inversion

In the time domain, the Laplace transform inverse of a function $\mathbb{Z}(x,s)$ can be written according to integral form with the Riemann sum approximation:

$$\mathbb{Z}(x,t') = \frac{1}{2\pi i}\int_{n-i\infty}^{n+i\infty} \exp(st\prime)\overline{\mathbb{Z}}(x,s)\mathrm{d}s = L^{-1}\{\overline{\mathbb{Z}}(x,s)\}. \tag{43}$$

However, equation (43) can be rewritten as

$$\mathbb{Z}(x,t') = \frac{\exp(nt')}{2\pi}\int_{\infty}^{\infty} e^{i\beta t}\overline{\mathbb{Z}}(x,n+i\xi)\mathrm{d}\xi. \tag{44}$$

The Fourier series expansion can be used on the interval $[0, 2t']$ for the function $\mathbb{Z}(x,s)$, which yields

$$\mathbb{Z}(x,t') = \frac{e^{nt'}}{t'}\left[\frac{1}{2}\overline{\mathbb{Z}}(x,n) + \mathrm{Re}\sum_{k=1}^{N}\overline{\mathbb{Z}}\left(x, n + \frac{ik\pi}{t'}\right)(-1)^n\right], \tag{45}$$

where $i = \sqrt{-1}$, $n \in R$ (real numbers), N is chosen freely, and the symbol Re expresses the real part and the notation $nt' \approx 4.7$ approximately [12]. Using the above numerical inversion technique, the final complete solutions of the mapped temperature, the strain, the holes carrier charge field, the carrier density, and the stress distribution are obtained.

On the other hand, the temperature distribution can be obtained from the temperature mapped according to the linearity as

$$\Theta = \frac{1}{K_0}\int_0^T K_0(1 + K_\theta T)\mathrm{d}T = T + \frac{K_\theta}{2}T^2 = \frac{K_\theta}{2}\left(T + \frac{1}{K_\theta}\right)^2 - \frac{1}{2K_\theta}. \tag{46}$$

In this case, the temperature distribution can be obtained in terms of Θ as

$$T = \frac{1}{K_\theta}\left[\sqrt{1 + 2K_\theta\Theta} - 1\right] \Leftrightarrow \overline{T} = \frac{1}{K_\theta}\left[\sqrt{1 + 2K_\theta\overline{\Theta}} - 1\right]. \tag{47}$$

6. Validation

6.1. The Photo-Thermoelasticity Models. The complete solutions are validated using comparisons with previous studies. Photo-thermoelasticity theories can be classified based on the various thermal and elastic memories. In this case, three models can be obtained, where τ_θ and τ_q are the first phase lag and the second heat flux phase-lag, respectively. The models can be classified as follows [30]:

(1) When $0 < \tau_\theta < \tau_q$, the dual phase lag (DPL) model is observed

(2) When $\tau_\theta = 0$, $0 < \tau_q$, the system is LS model

(3) When $\tau_\theta = \tau_q = 0.0$, the CT model is obtained

6.2. Magnetic Field Impact. When $H_0 = 0$, the Hall current impact and Hartmann number are ignored and the photo-thermoelasticity theory with holes and electrons interaction is obtained with variable thermal conductivity [31].

6.3. Variable Thermal Conductivity for Thermoelasticity Theory and the Hall Effect. The thermoelasticity theory only for the elastic medium is obtained under Hall current's influence and variable thermal conductivity when the influence of electron and hole are ignored ($N = 0$ and $H = 0$). Given this, the main governing equations are reduced to the following equations with Hall current and variable thermal conductivity [32]:

$$\begin{aligned}&\left\{\left(1 + \tau_\theta\frac{\partial}{\partial t}\right)\frac{\partial^2}{\partial x^2} - \left(1 + \tau_q\frac{\partial}{\partial t}\right)\frac{\partial}{\partial t}\right\}\Theta - \left(1 + \tau_q\frac{\partial}{\partial t}\right)\varepsilon_1\frac{\partial e}{\partial t} = 0,\\ &\left(\frac{\partial^2}{\partial x^2} - \frac{\partial^2}{\partial t^2} - \frac{M}{1 + m^2}\frac{\partial}{\partial t}\right)e - \left(1 + \tau_\theta\frac{\partial}{\partial t}\right)\frac{\partial^2\Theta}{\partial x^2} - \left(\frac{\sigma_0\mu_0^2H_0^2}{1 + m^2}\right)\frac{\partial e}{\partial t}.\end{aligned} \tag{48}$$

6.4. Magneto-Photo-Thermoelasticity Model with Changing the Thermal Conductivity. When the holes carrier charge field (holes carrier density) vanishes, i.e., $H = 0$, then a strong magnetic field with varying thermal conductivity is used to investigate the generalized photo-thermoelasticity theory. However, the governing equations are reduced to the equations as follows [33]:

$$\begin{aligned}
&\left\{\left(1+\tau_\theta\frac{\partial}{\partial t}\right)\frac{\partial^2}{\partial x^2}-\left(1+\tau_q\frac{\partial}{\partial t}\right)\frac{\partial}{\partial t}\right\}\Theta+\left\{\alpha_1\frac{\partial^2}{\partial x^2}-\alpha_2\left(1+\tau_q\frac{\partial}{\partial t}\right)-\alpha_3\frac{\partial}{\partial t}-\alpha_4\right\}N=\left(1+\tau_q\frac{\partial}{\partial t}\right)\varepsilon_1\frac{\partial e}{\partial t}\Bigg\},\\
&\left\{\frac{\partial^2}{\partial x^2}-\alpha_8\frac{\partial}{\partial t}\right\}\Theta+\left\{\alpha_9\frac{\partial^2}{\partial x^2}-\left(\alpha_{10}+t^n\frac{\partial}{\partial t}\right)\alpha_{11}+\left(1+t^n\frac{\partial}{\partial t}\right)\frac{\alpha_{11}}{t^n}\right\}N=\alpha_{13}\frac{\partial e}{\partial x},\\
&\left(\frac{\partial^2}{\partial x^2}-\frac{\partial^2}{\partial t^2}-\frac{M}{1+m^2}\frac{\partial}{\partial t}\right)e-\left(1+\tau_\theta\frac{\partial}{\partial t}\right)\frac{\partial^2\Theta}{\partial x^2}-\frac{\partial^2 N}{\partial x^2}-\left(\frac{\sigma_0\mu_0^2H_0^2}{1+m^2}\right)\frac{\partial e}{\partial t}.
\end{aligned}\tag{49}$$

6.5. The Impact of Thermal Conductivity. The thermal conductivity is independent of the temperature, in case of $K = K_0$ and $K_\theta = 0$. Then, the problem is investigated according to GPTET with Hall's current impact. In this case, the system of equations is reduced as [34]

$$\begin{aligned}
&\left(\left(1+\tau_\theta\frac{\partial}{\partial t}\right)\frac{\partial^2}{\partial x^2}-\left(1+\tau_q\frac{\partial}{\partial t}\right)\frac{\partial}{\partial t}\right)T+\left(\alpha_1\frac{\partial^2}{\partial x^2}-\alpha_2\left(1+\tau_q\frac{\partial}{\partial t}\right)-\alpha_3\frac{\partial}{\partial t}-\alpha_4\right)N+\left(\alpha_5\frac{\partial^2}{\partial x^2}-\left(1+\tau_\alpha\frac{\partial}{\partial t}\right)\alpha_6-\alpha_7\right)H=\left(1+\tau_q\frac{\partial}{\partial t}\right)\varepsilon_1\frac{\partial e}{\partial t}\Bigg\},\\
&\left\{\frac{\partial^2}{\partial x^2}-\alpha_8\frac{\partial}{\partial t}\right\}T+\left\{\alpha_9\frac{\partial^2}{\partial x^2}-\left(\alpha_{10}+t^n\frac{\partial}{\partial t}\right)\alpha_{11}+\left(1+t^n\frac{\partial}{\partial t}\right)\frac{\alpha_{11}}{t^n}\right\}N-\alpha_{12}\frac{\partial H}{\partial t}-\alpha_{13}\frac{\partial e}{\partial t}=0\Bigg\},\\
&\left\{\frac{\partial^2}{\partial x^2}-\alpha_{18}\frac{\partial}{\partial t}\right\}T+\left\{\alpha_{14}\frac{\partial^2}{\partial x^2}-\left(\alpha_{15}+t^h\frac{\partial}{\partial t}\right)\alpha_{16}\frac{\partial}{\partial t}+\left(1+t^h\frac{\partial}{\partial t}\right)\alpha_{17}\right\}H-\alpha_{19}\frac{\partial N}{\partial t}-\alpha_{20}\frac{\partial e}{\partial t}=0\Bigg\},\\
&\left[\frac{\partial^2}{\partial x^2}-\frac{\partial^2}{\partial t^2}-\frac{M}{1+m^2}\frac{\partial}{\partial t}\right]e-\left(1+\tau_\theta\frac{\partial}{\partial t}\right)\frac{\partial^2 T}{\partial x^2}-\frac{\partial^2 N}{\partial x^2}-\alpha_{21}\frac{\partial^2 H}{\partial x^2}=0.
\end{aligned}\tag{50}$$

7. Numerical Outcomes and Discussion

This section investigates the wave propagations in the semiconductor medium by numerically simulating the primary physical fields (temperature, tension, holes charge carrier field, and plasma (carrier density) distributions). For that, silicon (Si) material's physical constants are employed. The parameters are utilized in the SI unit and are listed in Table 1 [34, 35]. To perform these simulations and explain them, we may use the Matlab program to graph the basic distribution of the fields.

7.1. The Photo-Thermoelasticity Models. The key physical field variations (thermal waves, thermal temperature, normal stress (mechanical waves), holes charge carrier field, and plasma waves (carrier density)) against the axial distance are computed numerically and graphed in three groups based on the silicon input parameters mentioned above (Figures 1 and 2). For a brief time = 0.0001, all calculations use dimensionless quantities. Following the methodology described in [35], the distance to the absorption boundary was determined by striking a balance between the necessary accuracy and the CPU time. Some numerical methods are used for solving the above system of equations. The coupled photo-thermoelasticity models are plotted in Figure 1 (first group) following the varied values of relaxation time (during the changing of thermal conductivity, $K_\theta = -0.8$) when the Hall current effect is present and the semiconductor medium relies on temperature. The first subfigure shows how dimensionless thermal waves begin at the free surface at zero point and meet the thermal boundary condition propagate against distance. The thermal waves rapidly increase near the outer surface until they reach the peak maximum point as a result of the absorbed optical energy and the Hall current action. The influence of the absorbed light energy and the strong magnetic field inside the material diminishes exponentially, reaching its minimum value and approaching the zero line before dissipating with increasing distance. The second subfigure illustrates how mechanical waves' (normal stress) distribution varies with distance using photo-thermoelasticity models. The distribution of mechanical waves starts at the edge of the positive value that satisfies the mechanical slope type condition. Due to the effects of the absorbed optical energy and the magnetic field, the distribution increases initially within the material for a short distance before it starts to gradually slope away from the surface until its convergence to the zero line (state of equilibrium). The hole carrier charge distributions begin with a positive value at the surface and quickly increase in accordance with the recombination processes to reach the maximum value due to the Hall current impact and thermal effect of the optical energy (the third subfigure). Moving away from the surface, the hole charge carrier distribution begins to gradually decrease in the form of an exponential wave until it approaches the state of stability near the zero line. In the fourth subfigure, the carrier density (plasma waves) against the axial distance according to the different photo-thermoelasticity models is shown. During the recombination processes, absorbed optical energy and a strong

magnetic field on the outer surface and the plasma waves start from a positive value and increase smoothly until they arrive at maximum values. On the contrary, the plasma waves begin to decrease gradually, moving away from the surface and spreading in the form of an exponential wave until they approach the zero line.

7.2. The Effect of Variable Thermal Conductivity. When the thermal conductivity of the semiconductor medium relies on temperature, the principal physical fields' fluctuations versus axial distance are shown in the second group (Figure 3). The computational results are made when $t = 0.0001$ s under the influence of Hall current according to the DPL model. When $K(T) = K_0(1 + K_\theta T)$, three cases are studied, which depend on the value of K_θ (in the range $-10^{-3} \leq K_\theta \leq 10^{-2}$ for the Si semiconductor medium) [30]. The first case $K_\theta = 0.0$ refers to the medium in an independent case of temperature, i.e., $K = K_0$. However, the other two cases, $K_\theta = -0.4$ and $K_\theta = -0.8$, define the situation in which the temperature affects the medium's thermal conductivity. According to different values K_θ, the amplitudes of the thermal wave, mechanical wave, hole charge carrier field, and plasma wave increase with increasing values K_θ.

7.3. The Results of Hall Current. The effect of the Hall current, which is connected to a strong magnetic field, on physical fields with T, σ, H, and N distributions in opposition to an increase in axial distance x is seen in the third group (Figure 2). According to the DPL model, all numerical computations are conducted during a brief time while the semiconductor medium is temperature-dependent. ($K_\theta = -0.8$) is understudy. According to the research of this group, semiconductors in the first case, the effect of the Hall current is ignored when the influence of the strong magnetic field is taken into account (the Hartmann number vanishes). In the second case, the impact of the Hall current caused by the magnetic field internal particles rearranges themselves in the presence of a strong magnetic field (Hall current). All physical quantity distributions especially the hole charge carrier distribution exhibit this.

7.4. The Effect of the Holes Carrier Charge Field. Figure 4 shows the wave propagation of the main physical fields versus the axial distance according to the DPL model with different values of variable thermal conductivity in the absence of holes carrier charge field. The magnitude of the temperature, displacement, normal stress, and carrier density distributions are found to increase in the first range near the outside surface to reach their maximum value as a result of all plasma, thermal, and mechanical loads. However, because of how the magnetic field and plasma-mechanical-elastic interact, the amplitude of the main physical fields increases as the variable thermal conductivity parameter increases.

8. Conclusion

A novel model in 1D deformation that takes into account the interaction between the electrons and holes is used to analyze the relationship between the plasma and thermoelastic waves. The innovative model was used to investigate the effect of a magnetic field, which exists along with the effect of Hall current when the medium is temperature dependent. Only a few reviews of the literature for this model were conducted due to the complexity of the idea when considering shifting thermal conductivity and coupling holes and electrons with the Hall current effect. The analysis of this model shows that the Hall current effect, variable thermal conductivity, and differences in thermal relaxation duration all have a significant impact on the propagation of waves in all physical fields. Some materials, particularly semiconducting ones, can have their physical properties altered by variations in the magnetic field and thermal conductivity. The effect of thermal memories, variable thermal conductivity, magnetic field, and the presence of gaps on surface waves is evident. This effect vanishes in the depth of semiconductors. The studies of Hall current and variable thermal conductivity are useful for scientists in elastic semiconductor media, especially the Hall sensor, Hall potentiometer, and electronics technology. This work can be used for numerous engineering processes relating to interface analysis and design, including the analysis and design of thermal resistance-coated materials.

Nomenclature

λ, μ:	Lame's elastic semiconductor parameters (N/m^2)
$\delta_n = (3\lambda + 2\mu)d_n$:	The deformation potential difference (Nm)
T_0:	Reference temperature in its natural state (K)
$\widehat{\gamma} = (3\lambda + 2\mu + k)\alpha_{t_1}$:	The volume thermal expansion (NK/m^2)
α_t:	The linear thermal expansion coefficient (K^{-1})
σ_{ij}:	The microelongational stress tensor (N/m^2)
ρ:	The density (kg/m^3)
α_{t_1}:	Coefficients of linear thermal expansion (K^{-1})
C_e:	Specific heat (J/(kg·K))
K:	The thermal conductivity ($W{\cdot}m^{-1}K^{-1}$)
τ^*:	The photogenerated carrier lifetime (s)
E_g:	The energy gap (eV)
n_0:	Electrons concentration at equilibrium
h_0:	Holes concentration at equilibrium
$\gamma = (3\lambda + 2\mu)\alpha_t$:	The thermal expansion coefficient (N/km^2)
α_h, α_n:	Thermo-diffusive parameters
τ_θ, τ_q:	The memories lag (s)
t^n, t^h:	The electron/holes relaxation time (s)
$\delta_h = (2\mu + 3\lambda)d_h$:	

	The hole elasto-diffusive parameter (Nm)
d_n:	The coefficients of electronic deformation (m^3)
d_h:	The hole deformation coefficients (m^3)
$m_{nq}, m_{qn}, m_{hq}, m_{qh}$:	Peltier-Dufour-Seebeck-Soret-like constants
D_n, D_h:	The diffusion coefficients of the electrons and holes (m^2/s)
$a_{Qn}, a_{Qh}, a_Q, a_n, a_h$:	The flux-like constants.

Data Availability

The data generated and/or analyzed during the current study can be obtained from the corresponding author upon reasonable request.

Conflicts of Interest

The authors declare that they have no conflicts of interest.

Acknowledgments

The authors extend their appreciation to the Deputyship for Research & Innovation, Ministry of Education, Saudi Arabia for funding this research work through the project no. QU-IF-2-3-3-27073. The authors also thank Qassim University for their technical support.

References

[1] E. Hall, "On a new action of the magnet on electric currents," *American Journal of Mathematics*, vol. 2, no. 3, pp. 287–292, 1879.

[2] M. A. Biot, "Thermoelasticity and irreversible thermodynamics," *Journal of Applied Physics*, vol. 27, pp. 240–253, 1956.

[3] H. Lord and Y. Shulman, "A generalized dynamical theory of thermoelasticity," *Journal of the Mechanics and Physics of Solids*, vol. 15, no. 5, pp. 299–309, 1967.

[4] A. E. Green and K. A. Lindsay, "Thermoelasticity," *Journal of Elasticity*, vol. 2, pp. 1–7, 1972.

[5] D. S. Chandrasekharaiah, "Thermoelasticity with second sound: a review," *Applied Mechanics Reviews*, vol. 39, no. 3, pp. 355–376, 1986.

[6] D. S. Chandrasekharaiah, "Hyperbolic thermoelasticity: a review of recent literature," *Applied Mechanics Reviews*, vol. 51, no. 12, pp. 705–729, 1998.

[7] J. N. Sharma, V. Kumar, and D. Chand, "Reflection of generalized thermoelastic waves from the boundary of a half-space," *Journal of Thermal Stresses*, vol. 26, no. 10, pp. 925–942, 2003.

[8] K. Lotfy and S. M. Abo-Dahab, "Two-dimensional problem of two temperature generalized thermoelasticity with normal mode analysis under thermal shock problem," *Journal of Computational and Theoretical Nanoscience*, vol. 12, no. 8, pp. 1709–1719, 2015.

[9] M. I. A. Othman and K. Lotfy, "The influence of gravity on 2-D problem of two temperature generalized thermoelastic medium with thermal relaxation," *Journal of Computational and Theoretical Nanoscience*, vol. 12, no. 9, pp. 2587–2600, 2015.

[10] B. Maruszewski, "Electro-magneto-thermo-elasticity of extrinsic semiconductors, classical irreversible thermodynamic approach," *Archives of Mechanics*, vol. 38, pp. 71–82, 1986.

[11] B. Maruszewski, "Electro-magneto-thermo-elasticity of extrinsic semiconductors, extended irreversible thermodynamic approach," *Archives of Mechanics*, vol. 38, pp. 83–95, 1986.

[12] B. Maruszewski, "Coupled evolution equations of deformable semiconductors," *International Journal of Engineering Science*, vol. 25, no. 2, pp. 145–153, 1987.

[13] J. N. Sharma and N. T. Thakur, "Plane harmonic elasto-thermodiffusive waves in semiconductor materials," *Journal of Mechanics of Materials and Structures*, vol. 1, no. 5, pp. 813–835, 2006.

[14] A. Mandelis, *Photoacoustic and Thermal Wave Phenomena in Semiconductors*, Elsevier, Amsterdam, Netherlands, 1987.

[15] D. Almond and P. Patel, *Photothermal Science and Techniques*, Springer Science & Business Media, Berlin, Germany, 1996.

[16] J. Gordon, R. Leite, R. Moore, S. Porto, and J. Whinnery, "Long- transient effects in lasers with inserted liquid samples," *Bulletin of the American Physical Society*, vol. 119, p. 501, 1964.

[17] K. Lotfy, "Effect of variable thermal conductivity during the photothermal diffusion process of semiconductor medium," *Silicon*, vol. 11, no. 4, pp. 1863–1873, 2019.

[18] K. Lotfy and R. S. Tantawi, "Photo-thermal-elastic interaction in a functionally graded material (FGM) and magnetic field," *Silicon*, vol. 12, no. 2, pp. 295–303, 2020.

[19] K. Lotfy, "A novel model of magneto photothermal diffusion (MPD) on polymer nano-composite semiconductor with initial stress," *Waves in Random and Complex Media*, vol. 31, no. 1, pp. 83–100, 2019.

[20] K. Lotfy, A. El-Bary, W. Hassan, and M. Ahmed, "Hall current influence of microtemperature magneto-elastic semiconductor material," *Superlattices and Microstructures*, vol. 139, Article ID 106428, 2020.

[21] A. Mahdy, K. Lotfy, M. Ahmed, A. El-Bary, and E. Ismail, "Electromagnetic Hall current effect and fractional heat order for microtemperature photo-excited semiconductor medium with laser pulses," *Results in Physics*, vol. 17, Article ID 103161, 2020.

[22] A. M. S. Mahdy, K. Lotfy, A. El-Bary, and I. M. Tayel, "Variable thermal conductivity and hyperbolic two-temperature theory during magneto-photothermal theory of semiconductor induced by laser pulses," *European Physical Journal-Plus*, vol. 136, no. 6, p. 651, 2021.

[23] A. M. S. Mahdy, K. Lotfy, A. El-Bary, and H. H. Sarhan, "Effect of rotation and magnetic field on a numerical-refined heat conduction in a semiconductor medium during photo-excitation processes," *European Physical Journal-Plus*, vol. 136, no. 5, p. 553, 2021.

[24] K. Lotfy, "A novel model for Photothermal excitation of variable thermal conductivity semiconductor elastic medium subjected to mechanical ramp type with two-temperature theory and magnetic field," *Scientific Reports*, vol. 9, no. 1, p. 3319, 2019.

[25] A. M. Megahed, M. G. Reddy, and W. Abbas, "Modeling of MHD fluid flow over an unsteady stretching sheet with thermal radiation, variable fluid properties and heat flux," *Mathematics and Computers in Simulation*, vol. 185, pp. 583–593, 2021.

[26] A. M. Megahed and M. G. Reddy, "Numerical treatment for MHD viscoelastic fluid flow with variable fluid properties and viscous dissipation," *Indian Journal of Physics*, vol. 95, no. 4, pp. 673–679, 2021.

[27] M. Gnaneswara Reddy and M. Ferdows, "Species and thermal radiation on micropolar hydromagnetic dusty fluid flow across a paraboloid revolution," *Journal of Thermal Analysis and Calorimetry*, vol. 143, no. 5, pp. 3699–3717, 2021.

[28] K. Ramesh, M. G. Reddy, and B. Souayeh, "Electro-magneto-hydrodynamic flow of couple stress nanofluids in micro-peristaltic channel with slip and convective conditions," *Applied Mathematics and Mechanics*, vol. 42, no. 4, pp. 593–606, 2021.

[29] M. Marin, "On weak solutions in elasticity of dipolar bodies with voids," *Journal of Computational and Applied Mathematics*, vol. 82, no. 1-2, pp. 291–297, 1997.

[30] M. Marin, "Harmonic vibrations in thermoelasticity of microstretch materials," *Journal of Vibration and Acoustics*, vol. 132, no. 4, Article ID 044501, 2010.

[31] I. A. Abbas and M. Marin, "Analytical solutions of a two-dimensional generalized thermoelastic diffusions problem due to laser pulse," *Iranian Journal of Science and Technology, Transactions of Mechanical Engineering*, vol. 42, no. 1, pp. 57–71, 2018.

[32] S. Mondal and A. Sur, "Photo-thermo-elastic wave propagation in an orthotropic semiconductor with a spherical cavity and memory responses," *Waves in Random and Complex Media*, vol. 31, 2020.

[33] I. A. Abbas, F. S. Alzahrani, and A. Elaiw, "A DPL model of photothermal interaction in a semiconductor material," *Waves in Random and Complex Media*, vol. 29, no. 2, pp. 328–343, 2019.

[34] A. M. S. Mahdy, "A numerical method for solving the nonlinear equations of Emden-Fowler models," *Journal of Ocean Engineering and Science*, 2022.

[35] J. Smajic, C. Hafner, K. Tavzarashvili, and R. Vahldieck, "Numerical analysis of channel plasmon polaritons enhanced optical antennas," *Journal of Computational and Theoretical Nanoscience*, vol. 5, no. 4, pp. 725–734, 2008.